Journal Pre-proof

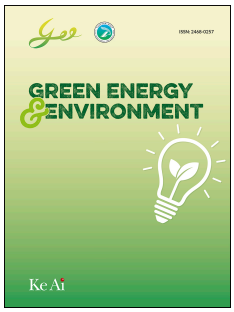

Application of deep learning for informatics aided design of electrode materials in metal-ion batteries

Bin Ma, Lisheng Zhang, Wentao Wang, Hanqing Yu, Xianbin Yang, Siyan Chen, Huizhi Wang, Xinhua Liu

PII: S2468-0257(22)00146-7

DOI: https://doi.org/10.1016/j.gee.2022.10.002

Reference: GEE 612

To appear in: *Green Energy and Environment*

Received Date: 9 August 2022

Revised Date: 29 September 2022

Accepted Date: 11 October 2022

Please cite this article as: B. Ma, L. Zhang, W. Wang, H. Yu, X. Yang, S. Chen, H. Wang, X. Liu, Application of deep learning for informatics aided design of electrode materials in metal-ion batteries, *Green Energy & Environment*, https://doi.org/10.1016/j.gee.2022.10.002.

Application of deep learning for informatics aided design of electrode materials in metal-ion batteries

Bin Ma[a,b], Lisheng Zhang[a], Wentao Wang[a], Hanqing Yu[a], Xianbin Yang[b], Siyan Chen[b], Huizhi Wang[c], Xinhua Liu[a,*]

[a] School of Transportation Science and Engineering, Beihang University, Beijing 102206, China

[b] College of Automotive Engineering, Jilin University, Changchun 130022, China

[c] Department of Mechanical Engineering, Imperial College London, London, SW7 2BX, UK

* Corresponding authors. School of Transportation Science and Engineering, Beihang University, Beijing 102206, China;

Email addresses:
Prof. Xinhua Liu Email: liuxinhua19@buaa.edu.cn.

Application of deep learning for informatics aided design of electrode materials in metal-ion batteries

Bin Ma[a,b], Lisheng Zhang[a], Wentao Wang[a], Hanqing Yu[a], Xianbin Yang[b], Siyan Chen[b], Huizhi Wang[c], Xinhua Liu[a,*]

[a] School of Transportation Science and Engineering, Beihang University, Beijing 102206, China

[b] College of Automotive Engineering, Jilin University, Changchun 130022, China

[c] Department of Mechanical Engineering, Imperial College London, London, SW7 2BX, UK

Abstract

To develop emerging electrode materials and improve the performances of batteries, the machine learning techniques can provide insights to discover, design and develop battery new materials in high-throughput way. In this paper, two deep learning models are developed and trained with two feature groups extracted from the Materials Project datasets to predict the battery electrochemical performances including average voltage, specific capacity and specific energy. The deep learning models are trained with the multilayer perceptron as the core. The Bayesian optimization and Monte Carlo methods are applied to improve the prediction accuracy of models. Based on 10 types of ion batteries, the correlation coefficients are maintained above 0.9 compared to DFT calculation results and the mean absolute error of the prediction results for voltages of two models can reach 0.41 V and 0.20V, respectively. The electrochemical performance prediction times for the two trained models on thousands of batteries are only 72.9 ms and 75.7 ms. Besides, the two deep learning models are applied to approach the screening of emerging electrode materials for sodium-ion and potassium-ion batteries. This work can contribute to a high-throughput computational method to accelerate the rational and fast materials discovery and design.

Keywords

Cathode materials; material design; electrochemical performance prediction; deep learning; metal-ion batteries

1 Introduction

The large-scale energy storage systems are extremely important for the utilization of renewable resources, such as wind, tidal and solar.[1,2] The electrochemical energy storage device could satisfy the emerging demand for different grid functions. Currently, the lithium-ion batteries (LIBs) have revolutionized the energy storage technology and are significantly important in transforming portable devices due to their high energy and power density, low cost and long lifetime.[3–5] However, it should be noted that the current LIBs suffer from several issues.[6,7] It's difficult for lithium ion to diffuse through the bulk phase of conventional transition metal oxides of cathodes. The transferability of traditional LIBs to higher energy scales remains a challenge.[8,9] Though the specific energy of conventional LIBs has almost reached the theoretical limitation, the performance and cost are not satisfactory. Therefore, great efforts need to be devoted to the discovery of new materials to further advance current battery technology.

The major technological advancement is largely driven by the exploration of new materials. On the one hand, material design focuses on the optimization of lithium batteries, including electrode materials, electrolytes, additives, etc. On the other hand, battery optimization is executed in the direction of other ion battery development. For LIBs or other ion

batteries in general, the design and discovery of electrode materials is critical. Tao et al. reviewed the researches of nonequilibrium ion transport in porous electrode with molecular and continuum methods. He prospected some insights for application of non-equilibrium thermodynamics in electrochemical system.[10] Zhang et al. highlighted an unsupervised learning scheme to screen all known Li-containing compounds.[11] Wang highlighted a method which can overcome the leakage problem of ionic liquids with the absence of encapsulation layers.[12] It's desirable to meet the following requirements in new electrode materials, including high cell voltages, enhanced power capacities, excellent charge and energy capacities and reliable safety, respectively.[13–16]

The material research in the past has significantly relied on either trial-and-error processes or chance discoveries, both of which require a large number of tedious experiments, causing a consumption of manpower, material resources and time. This method and exploration mode could require decades of research to identify a suitable material and a longer time to optimize for the final commercialization. A scalable approach is urgently needed to predict, screen and optimize materials at an unparalleled scale and rate. The computational chemistry, such as first-principles calculations[17], quantum mechanics, molecular dynamics[18] and Monte Carlo techniques[19], has been developed to complement and assist experimental researches for new materials discovery. The computational chemistry, represented by density functional theory (DFT) methods, has made significant progress in many areas. Enabled by the significant improvement in computing architectures, the DFT predictions do provide reasonable insights and can be applied to guide experimental research.[20] Furthermore, sufficient DFT computing experiments can contribute to the formation of well-curated and verified databases. However, in some context, they have not established a relationship between material design and electrode performance, and their calculations can take tens or hundreds of hours, leading to limit of applications in high-throughput screening.

The combination of artificial intelligence with big data is considered as "the fourth paradigm of science". With the machine learning as core part of artificial intelligence, statistical law could be found to produce reliable, repeatable decisions behind high-dimensional data. Benefiting from a rich library of datasets for describing molecular structures, the integration of traditional computational materials science with artificial intelligence technology, such as databases, data-mining and machine learning methods, has begun to emerge. The conventional methods could be utilized to determine model inputs and further speed up model development. Extensive data sets of materials properties have been compiled based on DFT or experiments, including Open Quantum Materials Database (OQMD)[21,22], Materials Project (MP)[23,24], Automatic FLOW (AFLOW)[25,26] and NOMAD[27]. These datasets have grown large enough that the discovery of new materials is impractical to accomplish by relying simply on human intuition and knowledge with battery mechanism.

The design routes of machine learning method for electrode materials are available in both forward and backward directions. The forward direction predicts performance from possible electrode materials and the backward direction could deduce battery materials from desired performance.[28–33] Currently, some machine learning models have successfully predicted the properties of battery materials, including support-vector machines (SVM), random forest (RF), logistic regression (LR) and recurrent neural network (RNN), etc. Joshi et al. developed a machine-learning model based on MP datasets to predict the average voltage of electrode materials and compare it to DFT calculations.[34] Ward et al. created a framework which could be applied to a broad range of materials data for accelerating the materials research and design.[35] The SVM and KRR models were utilized to obtain the possible reactions and thermal stability of interfaces.[36] Ibrahim et al. developed a Bayesian neural network (BNN) to predict the ionic conductivity of polymer electrolyte with the inputs of chemical compositions and temperatures.[37] Sarkar et al. applied multilayer perceptron to predict the average voltage of cathode materials with the input of central atom electronegativity.[38] Seko et al. predicted the cohesive energy of binary and ternary compounds, thermal conductivity of binary inorganic compounds with the usage of support vector regression.[39,40] Sendek et al. utilized the logistic regression to construct a data-driven ionic conductivity classification model, screening out 21 structures from 12831 lithium containing crystalline solids.[41] Though these models demonstrate the promise of machine learning methods in new materials discovery, they only cover a little fraction of the properties that could be utilized in materials design. Besides, though some large-scale databases have existed for years, there are no corresponding widely applicable and

machine-learning-based models. Overall, machine learning technology is an important means of making rational use of the current large datasets and is a promising technique for aiding DFT and experiments.

In this paper, a high-throughput screening method based on deep learning method is developed for predicting key electrochemical performance properties such as voltage, specific capacity and specific energy. We have built two feature sets and further constructed two models, where model #1 can work independently and model #2 has a higher accuracy, and both of them can predict three properties simultaneously. This method can contribute to the screening and design of electrode materials in two ways. Firstly, when the accuracy of deep learning model is obviously lower than theoretical calculation, it can be performed in series with theoretical calculation. The deep learning model can obtain complex correlations and patterns from the mass existing data and provide a solution to the rapid screen of materials. After initial screening with fast deep learning model, the exact calculation can be carried out by theoretical calculation. Secondly, when the accuracy of deep learning model is high enough, it can complete part of the calculation and obtain the prediction results directly in combination with the theoretical calculation.

2 Methodology

The dataset, model construction & training and error analysis are a few key components of deep learning method. In this section, they are described in detail on the purposed battery performance prediction.

2.1 Materials data analysis and pre-processing

In this paper, the datasets from MP are utilized for model training and testing. The MP is a component of the Materials Genome Initiative, which is mainly obtained by DFT calculations and could construct a collaborative material information resource for accelerated materials design. The MP could provide access to the data in a flexible and innovative way with multiple channels to visit its large and rich materials dataset. The MP adopts the open source software development to construct the collaborative platforms to help researchers to leverage on the expertise of the entire materials research community. In general, the MP provides material scientists with new angles to address the materials discovery issues, combining high-throughput computation, internet-based communication and open-source analysis methods.

The MP application programming interface (API), “mp_api”, is utilized to download the datasets. The downloaded data contains 10 types of ion batteries, including 2411 groups of Li-ion batteries data, 434 groups of Ca-ion batteries data, 33 groups of Cs-ion batteries data, 102 groups of potassium-ion batteries data, 417 groups of Mg-ion batteries data, 307 groups of sodium-ion batteries data, 45 groups of Rb-ion batteries data, 93 groups of Y-ion batteries data, 95 groups of Al-ion batteries data and 364 groups of Zn-ion batteries data, respectively. Each group contains the average voltage, specific capacity, specific energy and other relevant properties from completely deintercalated to fully intercalated ions.

In deep learning-based material property prediction, the purpose of selecting a set of input features is to create a collection of data that both uniquely defines a particular material and has a high correlation with the desired predicted property, and the deep learning method is essentially about capturing and describing this correlation. In this paper, the deep learning method is desired to describe the correlation between cathode materials and battery dynamic performance. Specifically, the electrode voltage, specific capacity and specific energy are predicted as the output of the deep learning model, using a set of characteristics that could represent the cathode materials.

According to the predicted objectives, four different attributes are extracted from the database as alternative input features, including stoichiometric attributes, crystal structure properties, electronic structure attributes and other battery attributes, respectively. The stoichiometric attributes include the types and proportions of elements contained in electrode materials at high-ion or low-ion states. The crystal structure properties are characterized by the regular three-dimensional periodic arrangement of atoms, ions and molecules in space such as the crystal lattice system and

space group number. The electronic structure attributes include the band gap, formation energy and Fermi level. The other battery attributes could include the types of ions, stability charge and stability discharge at high-ion and low-ion states. It should be noted that the alternative characteristics selected in this paper are only a small part of the total material properties and should not be considered as a complete set of properties describing the electrode material.

Based on these alternative features, two sets of input features are obtained in this paper. The set 1 uses only stoichiometric attributes, crystal structure properties and ionic species, which are relatively easy to obtain with no need to rely on experiments or extensive calculations. The purpose of using this set for model training is to develop a deep learning model that uses only simple input features. This model could not require first principles based on the theoretical calculations or experiments and allows for relatively independent, efficient and rapid initial predictions of battery electrochemical performance. Then the filtering of a large number of alternative materials is completed and the number of theoretical calculations could be reduced. The set 2 contains all the alternative features described above. The deep learning models trained with this set could not work independently because they contain properties such as band gap, stability, etc., which are obtained from theoretical calculations. The usage of this set is to provide a deep learning model that could use more inputs and is able to fully exploit and analyze the available database resources for the screening and performance prediction of novel battery materials in combination with theoretical calculations.

Before the features are imported into the deep learning model, they also need to be pre-processed. The utilized features and the corresponding pre-processing methods for two models are shown in Table 1.

Table 1. The pre-processing of input features

Input features	Used by model	Pre-processing
Formula	#1, #2	manual coding + principal component analysis + min-max normalization
Crystal lattice	#1, #2	one-hot coding
Space group	#1, #2	one-hot coding + principal component analysis
Ion type	#1, #2	one-hot coding
Formation energy	#2	min-max normalization
Band gap	#2	min-max normalization
Fermi level	#2	min-max normalization
Stability	#2	min-max normalization
Energy per atom	#2	min-max normalization

The pre-processing of the input features mainly includes three methods, manual coding, principal component analysis and min-max normalization. The manual coding simulates the one-hot coding method to distinguish between different chemical formulas. The principal component analysis is commonly used for dimensionality reduction of high-dimensional data and could be used to extract the main feature components of the data. The min-max normalization method could preserve the relationships between the original data and allow the data to fall into specific intervals. The pre-processing of formula charge and formula discharge consists of the three steps mentioned above. Fig. 1 demonstrates the processing flow for manual coding and principal component analysis. Manual coding is used to decompose the formulas into element types and atomic numbers. The formulas are coded according to the Periodic Table of Elements and all formulas are decomposed into 118 items. Principal component analysis can reduce the number of input features as to reduce the input noise so that the cumulative contribution rate is 0.99 and the 118 features can be downsized and reduced to 13 features. The dimensionality degradation requires the removal of some dimensional data, and naturally corresponding information is lost. We should minimize the loss of information as much as possible while reducing the dimensionality. The “f1, f2, f3, …” are the results of features after principal component analysis. They no longer have a specific physical meaning but correlate with features from before the dimensionality degradation. The min-max normalization could convert the number of atoms in each element of the formula into a proportion of each element and ensure that the weights of the different elements are consistent.

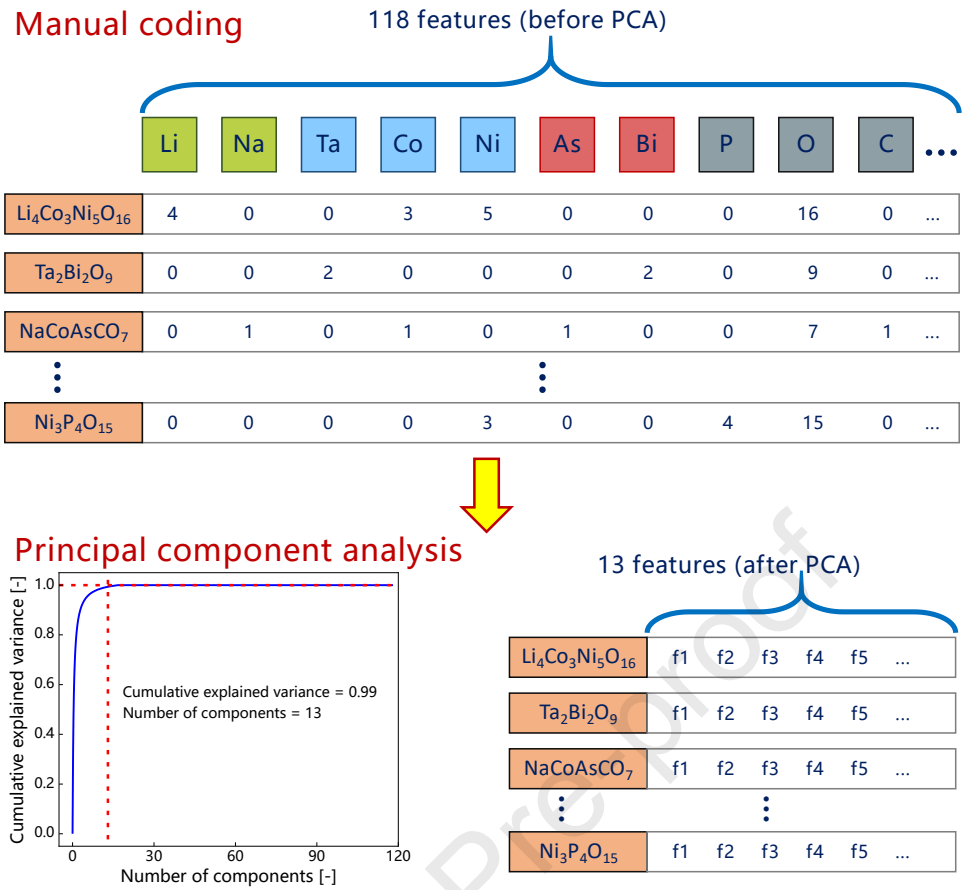

Fig. 1 The pre-processing of the dataset: manual coding for formulas and principal component analysis for the whole input features

2.2 Model construction and training

Ignoring the influence of electrolyte, separator and other battery materials, the performance of power battery, corresponding to each cathode material, could be approximately derived from the properties of this cathode material. It could be described as follows:

$$y_i = f(x_i) \tag{1}$$

Where y_i represents the electrochemical performance of each cathode material and x_i represents the properties of each cathode material. Obviously, there is no intersection between the different materials so that a feed forward network could be utilized to construct the deep learning model. Therefore, we use a classical deep learning method, the multilayer perceptron (MLP), to construct a prediction model for battery electrochemical performance.

Fig. 2 demonstrates the specific model structure, including input layer, dense layers and dropout layers. The input layer is responsible for the input of the entire model, whose inputs are the selected feature groups 1 & 2. These features are pre-processed with manual coding, one-hot coding, principal component analysis and min-max normalization.

In addition to the input and output layers, the MLP used in this paper has three hidden layers to capture the non-linear relationship between the selected input features and the predicted output. The output layer has three nodes corresponding to the average voltage, specific capacity and specific energy respectively.

During the training process, the root mean square prop (RMSprop) algorithm, the Bayesian optimization method and the Dropout techniques are utilized to improve the model performances.

The RMSprop algorithm is utilized to train the model, which can optimize the direction of the gradient update. It can enable adaptive adjustment of the learning rate, with the learning rate on the more variable gradient components

automatically decreasing and the learning rate on the less variable gradient components automatically increasing. The convergence speed and convergence character could be improved with RMSprop technique utilized to train the model. The selection of hyperparameters for deep learning model has a significant impact on both its training process and final prediction performance. In this paper, the Bayesian optimization approach is used to automatically optimize the model hyperparameters and thus the final prediction performance. The selected Bayesian optimization hyperparameters include the learning rate of the whole model, the number of nodes in the first three Dense layers and the discard rate of all three Dropout layers. The optimal hyperparameter values are calculated as follows:

$$d^* = argminJ(d), D \in (d_{min}, d_{max}), (d \in D) \tag{2}$$

Where d represents the hyperparameter value, d^* the optimal value and (d_{min}, d_{max}) the interval of optimization. There is a certain amount of uncertainty in the training process of the model due to the random weight initialization and the random discard of the Dropout layer, resulting in slight differences in the results of multiple training and predictions, which could be quantified using the Monte Carlo (MC) method. The MC method allows the confidence level to be obtained when the battery electrochemical performance is predicted by the constructed model, both of which are essential for the evaluation of model performance. The black-box function of MC can be described as follows:

$$\widehat{Q_{(J)}} = MODEL_i(x_{(j)}) \tag{3}$$

Where $\widehat{Q_J}$ represents the predicted capacity, $MODEL_i(\cdot)$ the specific utilized model.

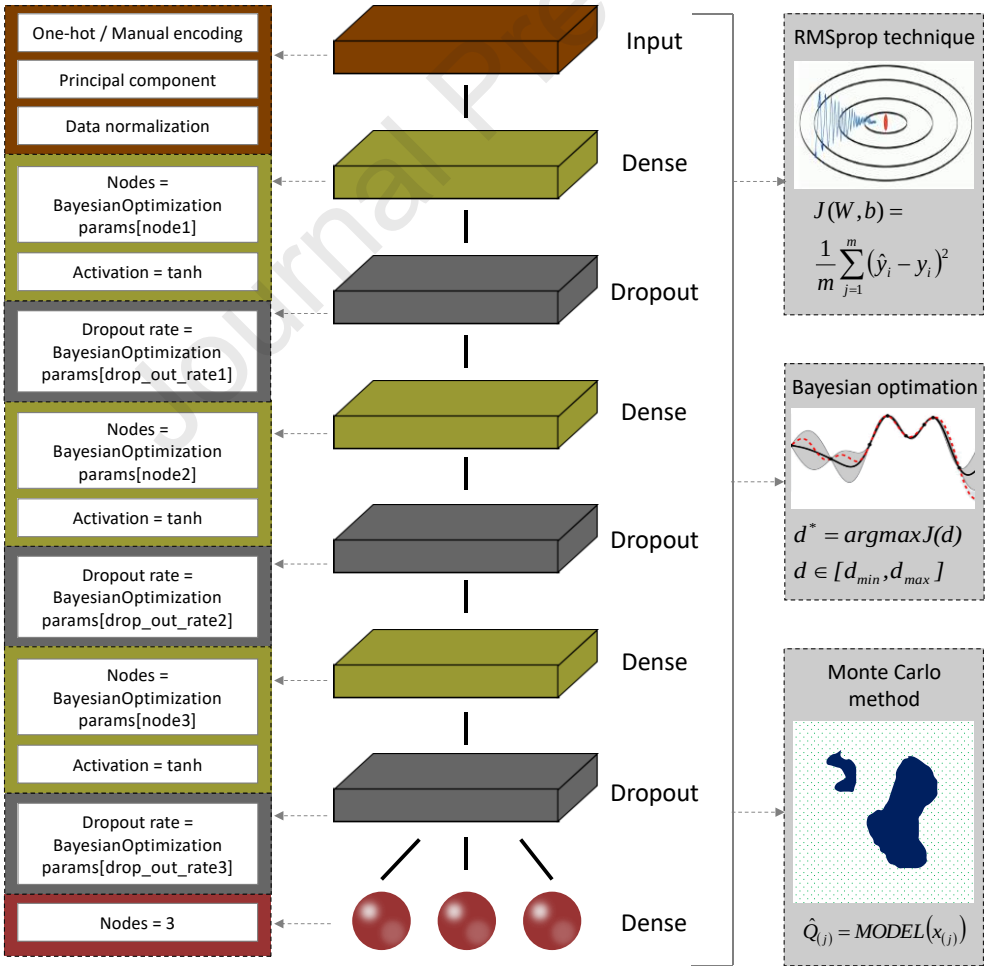

Fig. 2 The framework of the deep learning model with the MLP network as the core

In this paper, the original dataset is divided into three parts, the training set, the validating set and the test set, with a division ratio of 8.1:0.9:1. The training and validating sets are employed for model training and accuracy validation, and the trained deep learning model is applied based on the testing set. The specific battery groups of the three datasets

are chosen randomly to obtain a training set of length 3483, a validating set of length 388 and a test set of length 429. The more detailed information of dataset and original codes for our model are provided in the supporting information. Besides, the raw files of the program (.ipynb format) and dataset (.csv format) are publicly available, which can refer to the supporting information.

2.3 Model evaluation metrics

After the model is constructed and applied, some model evaluation metrics are utilized to evaluate the prediction results. In this paper, five metrics are applied, including the mean absolute error (MAE), the root mean square error (RMSE), the Pearson correlation coefficient, 95% confidence interval and the distribution of error.

The MAE indicates the mean of the absolute error between the predicted and observed values. It could be described as follows:

$$MAE = \frac{1}{N}\sum_{i=1}^{N}|y_i - \hat{y}_i^*| \tag{4}$$

Where the parameter MAE is the value for analysis of the prediction results. The y_i and $\hat{y}_i^*$ are the actual measured values and predicted values, respectively.

The RMSE represents the sample standard error between the predicted and observed values. It could be calculated as follows:

$$RMSE = \sqrt{\frac{1}{N}\sum_{i=1}^{N}(y_i - \hat{y}_i^*)^2} \tag{5}$$

Where $RMSE$ is the corresponding value for analysis of the prediction results, the y_i and $\hat{y}_i^*$ are the actual measured values and predicted values, respectively.

The Pearson correlation coefficient, is known as the Pearson product-moment correlation coefficient, could be utilized to measure the correlation between two variables. The formula could be described as follows:

$$r_{xy} = \frac{\sum_{i=1}^{n}(x_i-\bar{x})(y_i-\bar{y})}{\sqrt{\sum_{i=1}^{n}(x_i-\bar{x})^2}\sqrt{\sum_{i=1}^{n}(y_i-\bar{y})^2}} \tag{6}$$

Where *n* represents the number of sample series, *x* and *y* respectively represent a variable, and $\bar{x}$ and $\bar{y}$ respectively denote mean values of *x* and *y*.

The 95% confidence intervals refer to multiple intervals where 95% of the intervals could contain the true values, the performance of electrode materials in this paper. It could be calculated as follows:

$$P(X_{min} \le X_{real} \le X_{max}) = 0.95 \tag{7}$$

$$X_{min} = \mu - 1.96\frac{\sigma}{\sqrt{n}}, X_{max} = \mu + 1.96\frac{\sigma}{\sqrt{n}} \tag{8}$$

Where X represents the prediction properties, such as voltage, capacity and energy, and μ and σ are the mean and variance of the probability distribution function obtained from n calculations using the Monte Carlo method, respectively.

The distribution of error could help us visually identify the number of samples with different magnitude error, reflecting the statistical pattern of this error.

3 Results and discussion

In this section, the accuracy of trained deep learning models is firstly validated. Then the trained models are applied to screen the ideal cathode materials for sodium and potassium ion batteries.

3.1 Validation of model accuracy

In this subsection, the proposed deep learning model is trained on the already divided training set, and the training process is performed with the DFT calculation results as the label values. The feature group #1 and #2 are utilized to train the deep learning model #1 and #2, respectively. Accuracy validation of deep learning models are executed based on validating set and a total of 6 comparison results are shown, that is, the comparison of predictions of voltage, specific capacity and specific energy for model #1 and #2, respectively, with DFT calculation results. Besides, an error analysis is performed on the six comparison results, giving the results of the error distribution, MAE and RMSE analysis.

The Bayesian hyperparameter optimization results for model #1 and #2 are shown in Table 2. It can be seen that both models have a high number of nodes in the Dense layer to accommodate the increase in the dimensionality of the input features due to both manual and one-hot coding pre-processing techniques.

Table 2. Hyperparameter selection of the deep learning models.

Items	Deep learning model #1	Deep learning model #2
Units of Dense layer 1	404	230
Rate of Dropout layer 1	0.162	0.245
Units of Dense layer 2	116	160
Rate of Dropout layer 2	0.207	0.247
Units of Dense layer 3	276	318
Rate of Dropout layer 3	0.254	0.343
Learning rate	0.000323	0.000529
Optimizer	RMSprop	
Loss	Mean squared error	
Epoch size	1000	
Monte Carlo calculation times	50	

The voltage of a battery is a key parameter to determine its electrochemical performance, reliability and safety, which together with the specific capacity determines the specific energy. The prediction of battery voltage using corresponding electrode materials could accelerate the screen and development of high performance electrode materials.

Fig. 3(a) and (b) show the predicted voltage results of the two models compared to the DFT calculations based on the training set and validating set. The purple data points are the training results and the green data points are the validation results. The blue line represents the ideal state where the model predictions are identical to the DFT calculations, which exist as a reference standard. In addition, the Pearson correlation coefficients between the model predictions and the DFT calculations are also presented. The closer the value is to the 1, the higher the prediction accuracy of the model. Fig. 3(c) and (d) show the error distribution of the model prediction results compared to the DFT calculation results. The purple bars correspond to error in training results and green bars to error in validation results. It should be noted that the MC methods are utilized to reduce and quantify the impact of uncertainty in the training process of deep learning models. The number of MC calculations is 50. The results are the average of 50 independent model training and prediction. Besides, consistent with the input, the prediction results shown here actually include electrochemical performance of 10 ion batteries, that is, the constructed model has the ability to achieve performance predictions for different ion batteries.

As shown in Fig. 3(a) and (b), both model #1 and #2 predict the voltage well compared with the DFT calculation results. The discrete points are distributed around the reference line and the correlation coefficients calculated on the validating

set can reach above 0.9. However, the results of both models in the high voltage interval will be smaller than the DFT calculations, as shown in the red marked area. This phenomenon may be due to the limited sample size available for training the model in the high voltage range, which is insufficient to support the model in capturing the complex patterns required to correctly predict voltage. We believe that it would help to improve the performance of the model in the high voltage region if more samples from this interval could be available. As shown in Figure 3(c) and (d), the error distributions of both models basically take the form of a Gaussian distribution. The mean value is close to 0 V, which again supports that both models could approach the prediction of voltage well.

Comparing the prediction accuracy of the two models, the scatter plot of the prediction results of model #2 is more concentrated towards the reference line, which means that model #2 is more accurate. Similarly, this result is validated by the correlation coefficients and the error distributions shown in Fig. 3(c) and (d). The correlation coefficient for the validating set of model #2 could reach 0.978 while the correlation coefficient for the validating set of model #1 is only 0.902. The error distribution of model #2 is narrower and steeper when the horizontal and vertical coordinates remain the same.

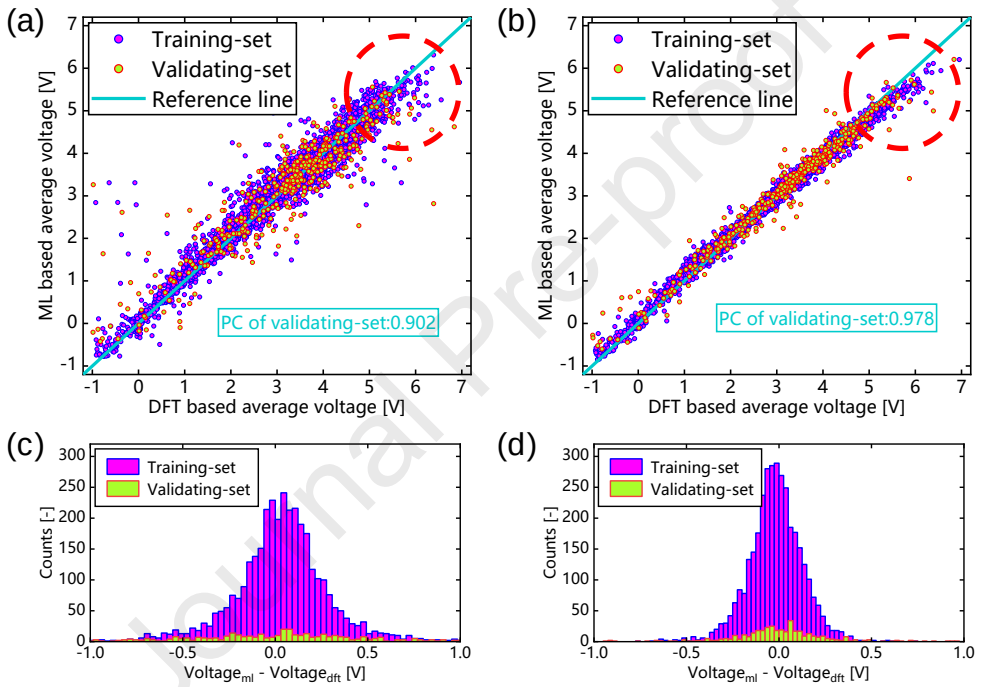

Fig. 3 The validation of the prediction results for average voltage. (a) The prediction results of average voltage from model #1 compared to DFT calculation results. (b) The prediction results of average voltage from model #2 compared to DFT calculation results. The error distribution of prediction results of (c) model #1 and (d) model #2.

The specific capacity of a battery is a key parameter to determine its electrochemical performance, and it could also be used to analyze battery reliability. Fig. 4 shows the predicted results of the two models on the training set and the validating set for the specific capacity compared to the results of the DFT calculation. It can be seen that the scatter points corresponding to both models are concentrated around the reference line and the error distribution are Gaussian with a mean value close to zero, which indicates that they can both achieve accurate predictions of the specific capacity. In addition, the two models have a higher accuracy in predicting the specific capacity compared to the voltage prediction, with correlation coefficients of 0.984 and 0.989 for the corresponding validating sets, respectively.

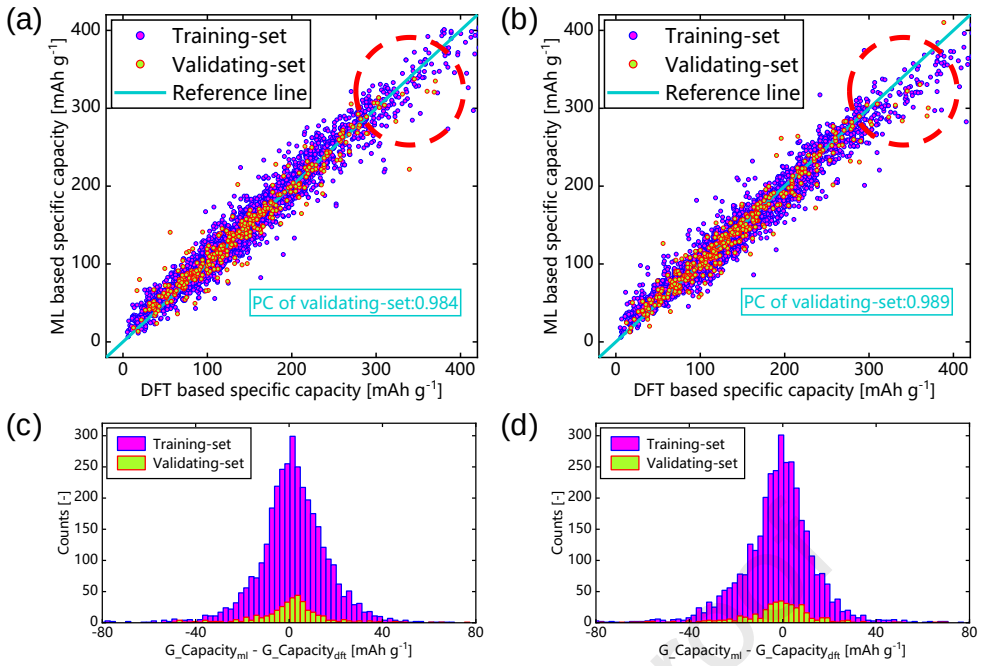

Fig. 4 The validation of the prediction results for specific capacity. (a) The prediction results of specific capacity from model #1 compared to DFT calculation results. (b) The prediction results of specific capacity from model #2 compared to DFT calculation results. The error distribution of prediction results of (c) model #1 and (d) model #2.

The specific energy is the most central parameter for measuring the electrochemical performance of a battery. Fig. 5 shows the comparison of the predicted specific energy results of the two models with the results of the DFT calculation. It can be seen that the prediction of specific energy by the constructed model is similar to that of voltage and specific capacity, that is, both models can complete the accurate prediction of battery specific energy, and the accuracy of model 2 is higher than that of model 1. The prediction accuracy of both models decreases in the high energy density interval, due to the small number of training samples in this interval.

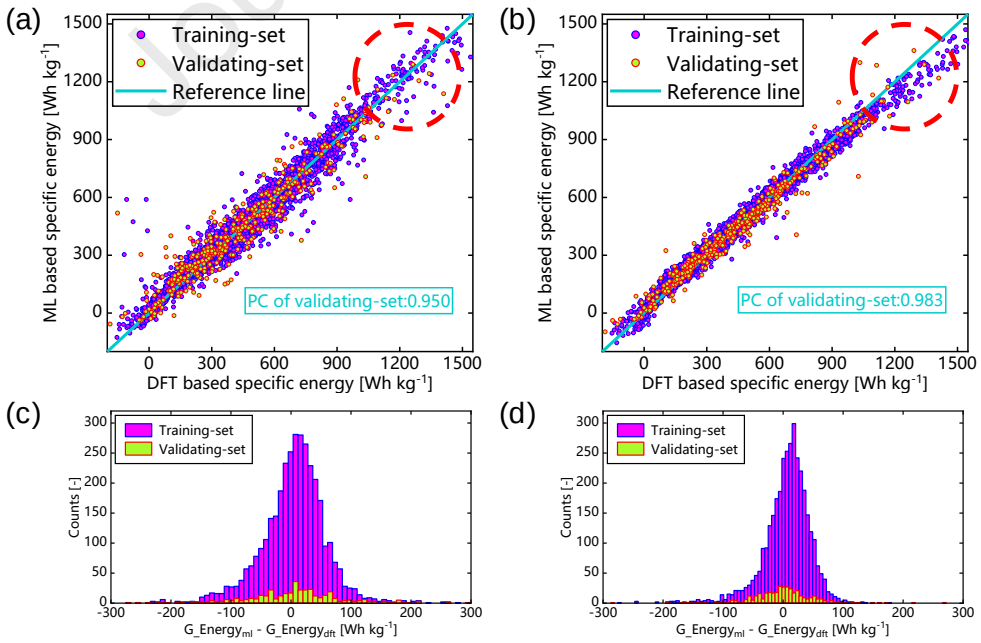

Fig. 5 The validation of the prediction results for specific energy. (a) The prediction results of specific energy from model #1 compared to DFT calculation results. (b) The prediction results of specific energy from model #2 compared to DFT calculation results. The error distribution of prediction results of (c) model #1 and (d) model #2.

Table 3 demonstrates the results of the quantitative evaluation of the constructed model in terms of two indicators, MAE and RMSE. Model #1 could predict the voltage, specific capacity and specific energy with the MAE of 0.4 V, 13 mAh g^{-1} and 66 Wh kg^{-1}, and the RMSE of 0.6 V, 30 mAh g^{-1} and 100 Wh kg^{-1}. It could be seen that the model #1 is accurate enough to support the initial screening of electrode materials. In contrast, the MAE and RMSE for voltage and specific energy predicted by model #2 are approximately half of those of model #1, and the MAE and RMSE for specific capacity are also lower than those of model #1. This is consistent with our expectation that the feature group #2 used in model #2 contains more complete and complex electrode material features than the feature group #1, as described in Section 2.1. The feature group #2 could provide more useful information for model training and prediction, and thus higher accuracy.

However, it should be noted that the input features used in model #2 include electronic properties of electrodes obtained by DFT calculations such as band gaps, which means that the model cannot work on its own even after the model has been trained and needs to be used in conjunction with theoretical calculations such as DFT to predict and screen the performance of new materials. Conversely, the feature group #1 used for model #1 only uses simple properties that are relatively easy to obtain such as crystal structure properties of the electrode material and stoichiometric properties. The model #1 could work independently of other theoretical calculations or experimental support after training, and achieve relatively good prediction accuracy. We believe that the application prospects of model #1 will be broader than model #2.

A comparison of the MC calculation results with the optimal single calculation results is shown in Table 3 as well. It can be seen that the accuracy of the MC calculation results is generally better than the optimal single calculation results. This is due to the fact that MC methods could not only quantify the uncertainty in the model training process, but also be utilized to achieve improved prediction accuracy in a way similar to ensemble learning. The MC methods used in this paper are calculated by first training the model with the training set 50 times. Due to the random initialization and Dropout layers, although the 50 models use the same hyperparameters and training set, the resulting weights are not the same for each node in each layer. That is, 50 relatively independent models are obtained. Afterwards, 50 models are applied to predict the battery electrochemical performance based on the validating set, so that 50 sets of voltage, specific capacity and specific energy prediction results are obtained for each electrode material, and then the final results are obtained by average weighting. In comparison, a single calculation can avoid the problem of the large computational effort required by the MC methods, but at the sacrifice of some model performance. We recommend that an appropriate balance between computational time and model performance can be achieved by wisely choosing the number of calculations in the MC methods.

Table 3. The results of the MAE and RMSE for validating set

	Items	**MC results of 50 times calculation**	**Best results in 50 times calculation**
Deep learning model #1	MAE - Voltage [V]	0.41	0.43
	MAE - G_Capacity [mAh g^{-1}]	13.38	14.54
	MAE - G_Energy [Wh kg^{-1}]	65.46	74.02
	RMSE - Voltage [V]	0.63	0.64
	RMSE - G_Capacity [mAh g^{-1}]	27.98	23.10
	RMSE - G_Energy [Wh kg^{-1}]	99.65	108.30
Deep learning model #2	MAE - Voltage [V]	0.20	0.21
	MAE - G_Capacity [mAh	13.01	15.87

g^{-1}]		
MAE - G_Energy [Wh kg^{-1}]	38.81	41.17
RMSE - Voltage [V]	0.32	0.32
RMSE - G_Capacity [mAh g^{-1}]	23.64	23.93
RMSE - G_Energy [Wh kg^{-1}]	61.21	62.22

In this paper, two feature groups are constructed and the feature group #2 contains more complete electrode material properties. Here in, feature group #2 is utilized to analyze the individual contributions of input features to evaluate their impact on prediction of battery electrochemical performances. The calculation can be described as follows:

$$Contribution_i = \frac{(PC_v+PC_c+PC_e)/3}{(PC_{v_i}+PC_{c_i}+PC_{e_i})/3} \quad (9)$$

Where $Contribution_i$ represents the individual contribution of the i^{th} input feature, PC_v, PC_c, PC_e the Pearson correlation coefficient between DFT calculation results and prediction results of average voltage, specific capacity and specific energy, respectively. PC_{v_i}, PC_{c_i}, PC_{e_i} represent the Pearson correlation coefficient between DFT calculation results and prediction results of average voltage, specific capacity and specific energy while the i^{th} input feature is removed, respectively. Obviously, if the contribution of an input feature is greater than 1, the absence of that input feature can lead to a decrease in model accuracy, and the larger the value, the greater the impact of the corresponding input feature.

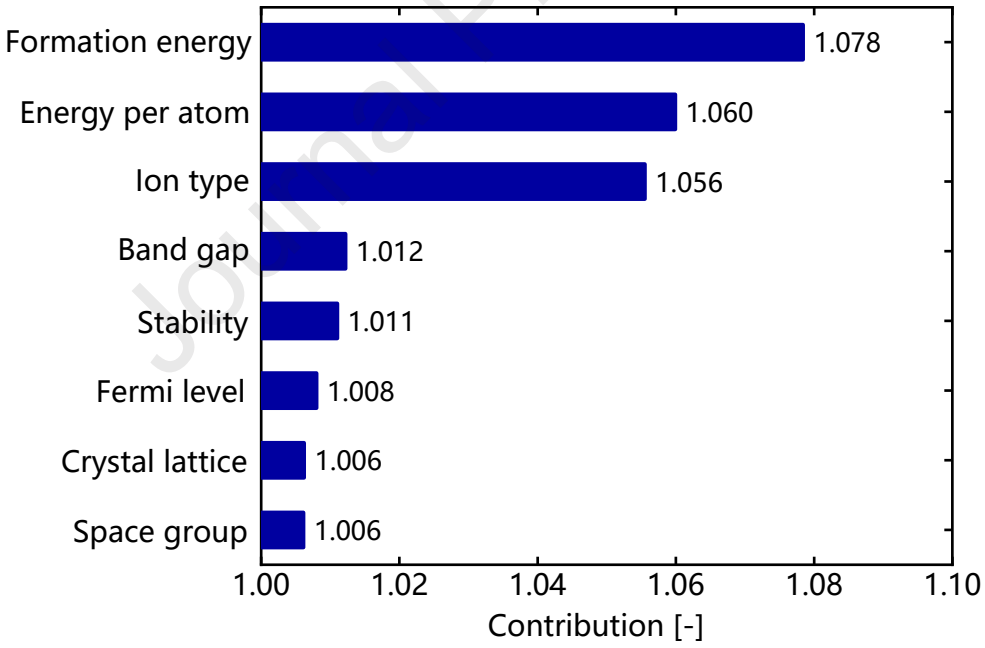

Fig. 6 evaluation of the individual contribution of input features

Fig. 6 shows the distribution of the calculated individual contributions for different input features. It can be seen that the contribution of all inputs is greater than 1, indicating that all these inputs have a positive impact on the improvement of the accuracy of the battery electrochemical performances prediction. Formation energy, Energy per atom and Ion type are the three input features with the highest contribution, while the other inputs have relatively low contribution. Besides, note that of all the input features, the chemical formula does not take part in the evaluation and by default has the highest individual contribution. In the absence of the chemical formula, the model will not work properly. Moreover, the Ion type shown in the figure is a relatively independent input feature in our model and its deletion does not have a direct impact on the chemical molecular formula.

Table 4 provides statistics on the computational time spent at different stages of model training and prediction. The

Bayesian optimization is performed on a training set containing 3483 cathode materials for hyperparameter search optimization, consisting of 30 iterations. The calculation time of model training and prediction are single computation times, which are averaged over 50 statistics.

The hardware computing platform is an NVIDIA A40 PCIe GPU with an acceleration frequency of 1740MHz and a base frequency of 1305MHz, a 48GB GDDR6 memory configuration, and a software computing environment of Python 3.8, Tensorflow 2.5.0 and Cuda 11.2.

Similar to deep learning modeling problems in other fields, model hyperparameter search and training time is large and increases with the number of samples and dimensionality of the input features However, when using the trained model for prediction, it consumes much less time. In this study, the single prediction computation time for both models are only 7.29 ms and 7.57 ms, while the computation time for DFT can typically be tens to hundreds of hours. By contrast, the proposed deep learning approach is more applicable to the problem of screening or performance prediction of high-throughput battery materials.

Table 4. Calculation time statistics of the proposed deep learning models.

Items	Calculation time of deep learning model #1	Calculation time of deep learning model #2	Computing platform	Remark
Bayesian optimization	6309.53 **s**	7354.65 **s**	NVIDIA A40	The total number of iterations for Bayesian optimization is 30 (3483 cathode material)
Model training	238.51 **s**	245.60 **s**		Mean of 50 statistics, training set (3483 cathode material)
Model validating	72.9 **ms**	75.7 **ms**		Mean of 50 statistics, validating set (388 cathode material)

Overall, based on the MP datasets, both deep learning models are able to achieve accurate predictions of the average voltage, specific energy and specific capacity using the corresponding electrode materials. The model trained using complex and complete feature groups as input could have a higher prediction accuracy. Both the two deep learning models could enable faster and easier material property prediction than the DFT calculation method without any significant degradation in prediction accuracy. Moreover, the constructed model is utilized to predict the average voltage based on data from other literature, and the detailed results are provided in the supporting information.

3.2 Application of model

Machine learning method can have wide applications in the field of materials, allowing for the discovery and design of new battery materials and large-scale screening and mathematical optimization of new materials with desired properties. In forward direction, the machine learning models can be constructed for prediction and screening. In backward direction, the inverse models can be obtained to predict the possible material structures with specific properties. During the training process of our model, the datasets contain 10 different metal ions, and the type of ion is also used as an input. Therefore, the model has the ability to predict the electrochemical performances of different ion batteries. In this subsections, two distinct applications for our novel material property prediction model are described in detail to demonstrate its practicality.

Application: Prediction and screening of new materials for sodium-ion batteries. To meet the increasing demands of vehicles electrification and smart power grids, the LIBs have been shown a sound output in high energy density, long life and eco-friendliness. However, the uneven distribution and the low affluence of lithium supplies doubt the development of efficient energy technologies. Though the specific energy of sodium-ion batteries is lower than that of LIBs, the sodium-ion batteries are still considered as one of the alternatives for LIBs due to their high abundance, high

safety and economic. The first application of our deep learning model is the establishment of a filter that could be used to screen cathode materials for sodium ion batteries. Similar to the filters provided by the MP website, a filter could give the desired primary screening result for the materials based on our constructed model. Specifically, we load each of 50 models generated by MC methods on the testing set for prediction, and then take the mean value as the final result. Then the sodium-ion battery cathode materials could be screened according to specific conditions.

Table 5 demonstrates the results obtained by screening in the testing set with the specific conditions, including "X-ion=sodium-ion && V⩾2 && C⩾100 && E⩾200". Then the screening results are compared with the results of filtering based on the DFT calculation. It could be seen that out of a total of 429 alternative materials, 9 are selected by DFT, 11 by model #1 and 10 by model #2. The two additional cathode materials that are screened by models are VO_2 and CrN_2. Table 6 demonstrates the prediction results for the two cathode materials. The 95% confidence intervals of the two materials are provided. The voltage and specific capacity of VO_2 and the voltage of CrN_2 predicted by the two deep learning models are lightly larger than the calculation results of DFT. Consequently, the two materials are screened by mistake. However, the efficiency of the deep learning models is significantly higher than that of DFT calculation methods with the reduction of the 429 candidate materials to a range of 11 candidates. Therefore, the deep learning model is sufficient for the primary screening of materials.

Table 5. The screening results of DFT and deep learning methods

Items	**results**
Filter criteria	x-ion = Na, average voltage ≥2 V, g_capacity ≥ 100 mAh g^{-1}, g_energy ≥ 200 Wh kg^{-1}
DFT	$Fe_3(PO_4)_4$, MnO_2, VPO_5, CuO_2, NiO_2, VP_2O_7, MnF_3, CoO_3, $FePO_4$
Deep learning model #1	$Fe_3(PO_4)_4$, MnO_2, VPO_5, CuO_2, NiO_2, VP_2O_7, MnF_3, CoO_3, $FePO_4$, **VO_2, CrN_2**
Deep learning model #2	$Fe_3(PO_4)_4$, MnO_2, VPO_5, CuO_2, NiO_2, VP_2O_7, MnF_3, CoO_3, $FePO_4$, **CrN_2**

Table 6. The prediction results of VO_2 and CrN_2

Items	**DFT**	**Deep learning model #1**	**Deep learning model #2**
X-ion		sodium-ion	
Formula		**$Na_3V_3O_6$ - VO_2**	
Average voltage [V]	1.84	2.32	2.09
95% Confidence interval	-	[2.29 - 2.35]	[2.07 - 2.12]
G_capacity [mAh g^{-1}]	98.6	112.3	98.3
95% Confidence interval	-	[110.2 - 114.3]	[96.4 - 100.2]
G_energy [Wh kg^{-1}]	181.3	254.2	218.5
Confidence interval	-	[248.4 - 259.9]	[214.6 - 222.5]
Formula		**$NaCrN_2$ - CrN_2**	
Average voltage [V]	1.96	2.30	2.55
95% Confidence interval	-	[2.18 - 2.42]	[2.51 - 2.59]
G_capacity [mAh g^{-1}]	260.2	207.9	188.5
95% Confidence interval	-	[200.6 - 215.3]	[182.3 - 194.6]

G_energy [Wh kg^{-1}]	511.0	476.4	495.8
Confidence interval	-	[449.7 - 503.1]	[480.5 - 511.1]

Application: Prediction of specific energy for potassium-ion batteries. In addition to sodium-ion batteries, potassium-ion batteries are also a promising alternative to Li-ion batteries. The potassium is nearly 1000 times more abundant that lithium in Earth's crust. Besides the low cost, the advantage of potassium-ion batteries is its excellent adaptability to the existing carbon industry which has been developed for LIBs. In this work, the Li in the testing set is replaced with potassium to predict the specific energy of potassium-ion batteries and the prediction results could be utilized to further guide the screening of the alternative cathode materials for potassium-ion batteries. Firstly, the specific energy of all Li-containing materials in the testing set is predicted and then the Li is replaced by K to predict the specific energy again. The predicted results are shown in Fig. 7. It could be seen that the predicted energy densities of potassium-ion batterie by two models are both lower than those of LIBs. Theoretically, the relative atomic mass of Li is less than that of K, which means that Li of the same mass could provide more electrons. Consequently, the specific energy of potassium-ion batteries is lower than LIBs, which is consistent with our prediction results.

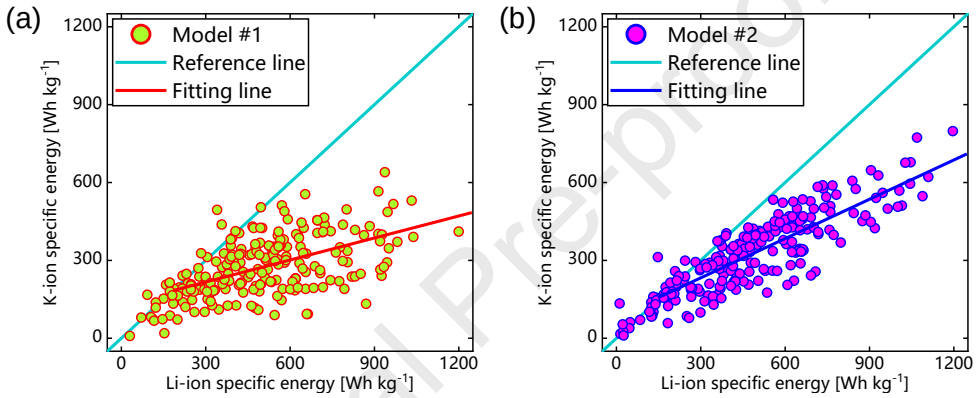

Fig. 7 The comparison of specific energy between the Li-ion batteries and potassium-ion batteries based on testing set for (a) model #1 and (b) model #2.

4 Conclusion

The rational design of materials is the ultimate goal of the exploration of emerging materials. However, there has been a gradual increase in the number of material datasets generated by the DFT calculation, experiments and other techniques and their size makes it difficult to process them simply based on the priori knowledge or experience of researchers. The DFT, as a typical computational approach of first principles, can obtain highly accurate computational results. However, it has a large computational overhead due to its computational complexity and "trial and error" character, causing a limited application in high-throughput computing field.

In this paper, two deep learning models, model #1 and model #2, are constructed and applied to establish a link between cathode materials and battery electrochemical performance. Firstly, the two feature groups are constructed and pre-processed with manual coding, principal component analysis and min-max normalization. Then the two feature groups are utilized to train two models for prediction of battery electrochemical performance, including voltage, specific capacity and specific energy. The results show that the two models could approach the accurate prediction of electrochemical performance of batteries with the correlation coefficients maintained above 0.9. Based on the training and validating sets, the constructed models are trained and validated with the MAE in voltage prediction of 0.41 V and 0.20 V, the MAE in specific capacity of 13.38 mAh g^{-1} and 13.01 mAh g^{-1}, and the MAE in specific energy of 65.46 Wh kg^{-1} and 38.81 Wh kg^{-1}, combined with Bayesian optimization and Monte Carlo methods. After the two deep learning models are constructed, trained and validated, they are applied to approach the screening of new materials,

such as electrode materials for sodium-ion batteries and potassium-ion batteries.

The trained model #1 could predict battery electrochemical performance independently with enough accuracy, not relying on theoretical calculations or experiments at all. The model #2, using the full and complete set of input features, could be utilized for deep mining current datasets with significantly higher accuracy. Overall, the model #1, using a simple set of input features, will have a much wider range of applications. Both the models developed in this work can predict the average voltage, specific capacity and specific energy simultaneously, thus enabling a more comprehensive prediction of battery electrochemical performance with a prediction calculation time of only tens of ms. Upon this foundation, it's promising that this work, combined with DFT calculation methods, can contribute to the discovery, design and development of emerging electrode materials for next-generation excellent performance batteries based on the ultra-high computational ability of cloud platform.

Acknowledgements

This work was financially supported by the National Natural Science Foundation of China (No. 52102470).

References

[1] G. Energy, Q. Li, J. Chen, L. Fan, X. Kong, Y. Lu, M. Goel, Y. Liu, Q. Sun, W. Li, K.R. Adair, J. Li, X. Zhang, Z. Xie, M.H. Yap, G.Z. Chen, J. Cen, Q. Wu, A. Orlov, Green Energy Environ. 4 (2019) 1–2.

[2] Q. Lu, Y. Jie, X. Meng, A. Omar, D. Mikhailova, R. Cao, S. Jiao, Y. Lu, Y. Xu, Carbon Energy 3 (2021) 957–975.

[3] G. Energy, P. Yang, X. Yang, W. Liu, R. Guo, Z. Yao, Green Energy Environ. (2022). https://doi.org/10.1016/j.gee.2022.06.008

[4] C. Duan, Y. Yu, J. Xiao, Y. Li, P. Yang, F. Hu, H. Xi, Green Energy Environ. 6 (2021) 33–49.

[5] X. Meng, Y. Xu, H. Cao, X. Lin, P. Ning, Y. Zhang, Y.G. Garcia, Z. Sun, Green Energy Environ. 5 (2020) 22–36.

[6] H. You, J. Zhu, X. Wang, B. Jiang, H. Sun, X. Liu, X. Wei, G. Han, S. Ding, H. Yu, W. Li, D.U. Sauer, H. Dai, J. Energy Chem. 72 (2022) 333–341.

[7] C. Lin, W. Kong, Y. Tian, W. Wang, M. Zhao, Automot. Innov. 5 (2022) 3–17.

[8] R.P. Joshi, B. Ozdemir, V. Barone, J.E. Peralta, J. Phys. Chem. Lett. 6 (2015) 2728–2732.

[9] K. Liu, Y. Liu, D. Lin, A. Pei, Y. Cui, Sci. Adv. 4 (2018). https://doi.org/10.1126/sciadv.aas9820

[10] H. Tao, C. Lian, H. Liu, Green Energy Environ. 5 (2020) 303–321.

[11] X. Zhang, B. Tang, Z. Zhou, Green Energy Environ. 6 (2021) 3–4.

[12] J. Wang, Green Energy Environ. 5 (2020) 122–123.

[13] J. Galos, K. Pattarakunnan, A.S. Best, I.L. Kyratzis, C.H. Wang, A.P. Mouritz, Adv. Mater. Technol. 6 (2021) 1–19.

[14] J. Mao, J. Miao, Y. Lu, Z. Tong, Chinese J. Chem. Eng. 37 (2021) 1–11.

[15] S. Zhao, Z. Guo, K. Yan, S. Wan, F. He, B. Sun, G. Wang, Energy Storage Mater. 34 (2021) 716–734.

[16] Y. Yang, Green Energy Environ. 5 (2020) 382–384.

[17] A. Ullah, A. Majid, N. Rani, J. Energy Chem. 27 (2018) 219–237.

[18] M. Endo, C. Kim, K. Nishimura, T. Fujino, K. Miyashita, 38 (2000) 183–197.

[19] R.N. Methekar, P.W.C. Northrop, K. Chen, R.D. Braatz, 158 (2011) 363–370.

[20] T.P. Kaloni, R.P. Joshi, N.P. Adhikari, U. Schwingenschlögl, Appl. Phys. Lett. 104 (2014). https://doi.org/10.1063/1.4866383

[21] J.E. Saal, S. Kirklin, M. Aykol, B. Meredig, C. Wolverton, Jom 65 (2013) 1501–1509.

[22] S. Kirklin, J.E. Saal, B. Meredig, A. Thompson, J.W. Doak, M. Aykol, S. Rühl, C. Wolverton, Npj Comput. Mater. 1

(2015). https://doi.org/10.1038/npjcompumats.2015.10

[23] S.P. Ong, S. Cholia, A. Jain, M. Brafman, D. Gunter, G. Ceder, K.A. Persson, Comput. Mater. Sci. 97 (2015) 209–215.

[24] A. Jain, S.P. Ong, G. Hautier, W. Chen, W.D. Richards, S. Dacek, S. Cholia, D. Gunter, D. Skinner, G. Ceder, K.A. Persson, APL Mater. 1 (2013). https://doi.org/10.1063/1.4812323

[25] S. Curtarolo, W. Setyawan, G.L.W. Hart, M. Jahnatek, R. V. Chepulskii, R.H. Taylor, S. Wang, J. Xue, K. Yang, O. Levy, M.J. Mehl, H.T. Stokes, D.O. Demchenko, D. Morgan, Comput. Mater. Sci. 58 (2012) 218–226.

[26] E. Gossett, C. Toher, C. Oses, O. Isayev, F. Legrain, F. Rose, E. Zurek, J. Carrete, N. Mingo, A. Tropsha, S. Curtarolo, Comput. Mater. Sci. 152 (2018) 134–145.

[27] C. Draxl, M. Scheffler, MRS Bull. 43 (2018) 676–682.

[28] S. Srinivasan, K. Rajan, C. Sciences, M.I. Collaboratory, (2013) 279–290.

[29] L.M. Ghiringhelli, J. Vybiral, S. V. Levchenko, C. Draxl, M. Scheffler, Phys. Rev. Lett. 114 (2015) 1–5.

[30] C.S. Kong, W. Luo, S. Arapan, P. Villars, S. Iwata, R. Ahuja, K. Rajan, J. Chem. Inf. Model. 52 (2012) 1812–1820.

[31] S. Yang, R. He, Z. Zhang, Y. Cao, X. Gao, X. Liu, Matter 3 (2020) 27–41.

[32] S. Yang, Z. Zhang, R. Cao, M. Wang, H. Cheng, L. Zhang, Y. Jiang, Y. Li, B. Chen, H. Ling, Y. Lian, B. Wu, X. Liu, Energy AI 5 (2021) 100088.

[33] X. Liu, L. Zhang, H. Yu, J. Wang, J. Li, K. Yang, Y. Zhao, H. Wang, B. Wu, N.P. Brandon, S. Yang, 2200889 (2022) 1–25.

[34] R.P. Joshi, J. Eickholt, L. Li, M. Fornari, V. Barone, J.E. Peralta, ACS Appl. Mater. Interfaces 11 (2019) 18494–18503.

[35] L. Ward, A. Agrawal, A. Choudhary, C. Wolverton, Npj Comput. Mater. 2 (2016) 1–7.

[36] B. Liu, J. Yang, H. Yang, C. Ye, Y. Mao, J. Wang, S. Shi, J. Yang, W. Zhang, J. Mater. Chem. A 7 (2019) 19961–19969.

[37] V. Nulu, A. Nulu, M.G. Kim, K.Y. Sohn, Int. J. Electrochem. Sci. 13 (2018) 5565–5574.

[38] T. Sarkar, A. Sharma, A.K. Das, D. Deodhare, M.D. Bharadwaj, Proc. IEEE Int. Caracas Conf. Devices, Circuits Syst. ICCDCS (2014) 12–14.

[39] A. Seko, H. Hayashi, K. Nakayama, A. Takahashi, I. Tanaka, Phys. Rev. B 95 (2017) 1–11.

[40] A. Seko, T. Maekawa, K. Tsuda, I. Tanaka, Phys. Rev. B - Condens. Matter Mater. Phys. 89 (2014) 1–9.

[41] A.D. Sendek, Q. Yang, E.D. Cubuk, K.A.N. Duerloo, Y. Cui, E.J. Reed, Energy Environ. Sci. 10 (2017) 306–320.

- Two feature groups that could be adapted to different application scenarios are constructed
- Two deep learning models are constructed to predict the electrochemical performances
- The performances prediction and screening of new materials for sodium-ion and potassium-ion batteries are executed
- The prediction times for two constructed model on thousands of cells reach 72.9 ms and 75.7 ms.

Declaration of interests

☒ The authors declare that they have no known competing financial interests or personal relationships that could have appeared to influence the work reported in this paper.

☐ The authors declare the following financial interests/personal relationships which may be considered as potential competing interests: